

Oscillations of α UMa and other red giants

W. A. Dziembowski^{1,2,3}, D. O. Gough^{1,4}, G. Houdek¹, R. Sienkiewicz³

¹*Institute of Astronomy, University of Cambridge, Cambridge CB3 0HA, UK*

²*Warsaw University Observatory, Al. Ujazdowskie 4, 00-478 Warsaw, Poland*

³*Copernicus Astronomical Center, Polish Academy of Sciences, ul. Bartycka 18, 00-716 Warsaw, Poland*

⁴*Department of Applied Mathematics and Theoretical Physics, University of Cambridge, Cambridge CB3 9EW, UK*

Accepted 2001 Received 2000 in original form

ABSTRACT

There is growing observational evidence that the variability of red giants could be caused by self-excitation of global modes of oscillation. The most recent evidence of such oscillations was reported for α UMa by Buzasi et al. (2000) who analysed space photometric data from the WIRE satellite.

Little is understood about the oscillation properties in red giants. In this paper we address the question as to whether excited radial and nonradial modes can explain the observed variability in red giants. In particular, we present the results of numerical computations of oscillation properties of a model of α UMa and of several models of a $2M_{\odot}$ star in the red-giant phase.

The red giant stars that we have studied have two cavities that can support oscillations: an inner core that supports gravity (g) waves and a surrounding shell that supports acoustic (p) waves. Most of the modes in the g-mode frequency range are g modes confined in the core; those modes whose frequencies are close to a corresponding characteristic frequency of a p mode in the outer cavity are of mixed character and have substantial amplitudes in the outer cavity. We have shown that such modes of low degree, $\ell = 1$ and 2, together with the radial (p) modes, can be unstable. The linear growth rates of these nonradial modes are similar to those of corresponding radial modes. In the model of α UMa and in the $2M_{\odot}$ models in the lower regions of the giant branch, high amplitudes in the p-mode cavity arise only for modes with $\ell = 2$.

We have been unable to explain the observed oscillation properties of α UMa, either in terms of mode instability or in terms of stochastic excitation by turbulent convection. Modes with the lowest frequencies, which exhibit the largest amplitudes and may correspond to the first three radial modes, are computed to be unstable if all effects of convection are neglected in the stability analyses. However, if the Lagrangian perturbation of the turbulent fluxes (heat and momentum) are taken into account in the pulsation calculation, only modes with higher frequencies are found to be unstable. The observed frequency dependence of amplitudes reported by Buzasi et al. (2000) does not agree with what one expects from stochastic excitation. This mechanism predicts an amplitude of the fundamental mode about two orders of magnitude smaller than the amplitudes of modes with orders $n \geq 5$, which is in stark disagreement with the observations.

Key words: stars: oscillations – stars: convection – stars: red giants

1 INTRODUCTION

Buzasi et al. (2000) have reported the discovery of oscillations in photometric data from α UMa observed with the star camera on the WIRE satellite. They interpret the observed oscillations as radial modes, and cautiously suggest that the modes may be excited by the mechanism similar to that responsible for solar oscillations. The star, however, is very different from the Sun. Its spectral type is K0 III. Mod-

els of the star's internal structure, and its pulsation properties, suggest that the star is a red giant. Thus, even if the oscillations are stochastically excited by turbulence in the outer convective zone, as they are in the Sun, some important differences between the oscillation properties of α UMa and the Sun should be expected.

Variability is a common feature of red giants. There are strong observationally based arguments that, at least in part, this variability is due to global pulsations. Edmonds

& Gilliland (1995) proposed radial or nonradial pulsations as an explanation for the variability they observed in K giants in the globular cluster 47 Tuc. They found frequencies between 3 and 6 μ Hz with amplitudes between 5 and 15 mmag. Cook et al. (1997) analysed photometric data from red stars in the LMC collected from the microlensing project MACHO, and reported that the period-luminosity relation comprises several ridges in the period range of 10–200-days, which may be interpreted as arising from radial modes of different n . Hatzes and Cochran (1998) reported that there is strong evidence from radial-velocity data for oscillations in K giants. Frequencies similar to those found in α UMa have been found in a number of other objects. In particular, Hatzes and Cochran quote 11 frequencies of Arcturus (K2 III) in the range 1.4–6.8 μ Hz. Evidence for short-period multimode pulsations in a number of M stars has been presented recently by Koen and Laney (2000).

Thus, by being a multimode pulsator α UMa appears not to be unique amongst red giants. But with its high frequencies and low amplitudes it does represent an extreme case so far, although it is not wholly out of line with the others. This star is the hottest and the least luminous object amongst variable red giants. It provides, so far, the best example of possible red-giant oscillations, but its spectrum is not as clean as that of the Sun, or of those of other main-sequence stars, or of white dwarfs. Nevertheless we consider the evidence to be strong enough to justify new investigations in the theory of red-giant oscillations. So far, only the modelling of radial pulsations in Miras (see Xiong et al. 1998 and references therein) and Arcturus (Balmforth et al. 1991) has attracted the theorists' attention. Nonradial oscillations in red giants have been ignored almost entirely. Here we review the theoretical aspects of this problem, in Section 3, and provide some numerical examples of the properties of the oscillations of a model of α UMa and of models of a $2 M_{\odot}$ star on the red-giant branch. Some data concerning these models are presented in Section 2.

The most intriguing issue posed by the discovery of oscillations in red giants is the identification of the mechanism by which they are driven. Possibilities to consider are (a) stochastic excitation of linearly stable modes by convection and (b) self-excitation of linearly unstable modes. We shall speak of oscillations of case (a) as being solar-like, and case (b), Mira-like. Our understanding of the excitation mechanism in the Sun and in Miras is not satisfactory, but the separate association of these stars with each of the two distinct possible excitation mechanisms is now generally accepted. In Section 4 we present results of calculations of radial-mode stability and of the amplitudes in the case of stochastic excitation.

2 SELECTED MODELS

There are stringent constraints on the parameters for defining models of α UMa. The star is bright, and is in a visual binary system. Accurate spectroscopic data, parallax, and a radius determination by means of interferometry are available. After considering all the observational data, Guenther et al. (2000) suggested the following values for the star's global parameters: $M=4-5 M_{\odot}$, $\log(L/L_{\odot}) = 2.5 \pm 0.05$, $T_{\text{eff}} = (4660 \pm 100)$ K. Guenther et al. (2000) constructed

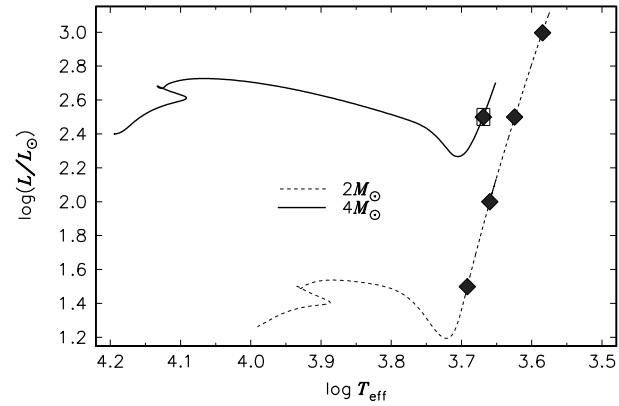


Figure 1. H-R diagram showing evolutionary tracks of models with masses of $2 M_{\odot}$ and $4 M_{\odot}$. Models selected for pulsation analyses are indicated by diamonds. The box around the symbol for the $4 M_{\odot}$ star indicates the uncertainty in locating α UMa in the diagram (see Table 1).

evolutionary models with masses in this range and with an initial chemical composition $X = 0.727$ and $Z = 0.0124$, which is consistent with the spectroscopic value of [Fe/H] and the Galactic helium enrichment. They found that only models with $M \leq 4.5 M_{\odot}$ satisfy the observational constraints.

We have adopted the same initial chemical composition in our model calculations. Furthermore, we have adopted the same opacity and equation of state. For the model of α UMa we have considered only $M = 4 M_{\odot}$, and we have adjusted the mixing-length parameter, α , to be consistent with the values of $\log(L/L_{\odot})$ and T_{eff} proposed by Guenther et al. (2000).

The star α UMa is a high-mass red giant with a non-degenerate core. Such stars are very rare. As seen in Fig. 1, the red-giant branch for $M = 4 M_{\odot}$ is very short; the star spends only 0.5 My on it, which is more than two orders of magnitude shorter than the time spent by a star with a mass of $M = 2 M_{\odot}$, in which helium ignites in a degenerate core. We have chosen the model sequence with $M = 2 M_{\odot}$ to illustrate nonradial mode properties in red giants over a wide range of luminosity. The most important parameter determining nonradial mode properties is the ratio of the mean density of the core to the mean density of the whole star. In the sequence we have chosen, this parameter increases by nearly four orders of magnitudes between the bottom and the top of the giant branch. We have considered four models for the $2 M_{\odot}$ sequence, calculated with the same values of X , Z and α as those for the model of α UMa. The locations of the selected models on the evolutionary tracks are indicated in Fig. 1; the parameters characterizing these models are listed in Table 1.

3 NONRADIAL MODES OF RED GIANTS

Guenther et al. (2000) considered only radial modes as potential candidates for explaining the peaks in the α UMa frequency spectrum determined by Buzasi et al. (2000). They noticed that the frequencies of these peaks are much lower than the buoyancy frequency deep in the star, and presumed that a nonradial interpretation would appear to imply that

Table 1. Some parameters of the models used in this work; M_c is the core mass including the hydrogen burning shell; the subscript bc denotes bottom of the convective envelope.

Model	M/M_\odot	age(Gy)	$\log T_{\text{eff}}$	$\log L/L_\odot$	R/R_\odot	$\log T_c$	$\log \rho_c$	M_c	r_{bc}/R	M_{bc}/M
M_α	4	0.143	3.6993	2.50	27.21	7.924	4.187	0.1083	0.3259	0.4300
M21	2	0.904	3.6915	1.50	7.77	7.753	4.766	0.1145	0.1481	0.1869
M22	2	0.934	3.6596	2.00	15.99	7.776	5.220	0.1397	0.0509	0.1527
M23	2	0.963	3.6240	2.50	33.50	7.780	5.555	0.1705	0.0264	0.1755
M24	2	0.972	3.5848	3.00	71.32	7.835	5.752	0.2017	0.0124	0.2042

the modes are g modes of high radial order. According to their estimate, the separation between the cyclic frequencies of consecutive g modes of like degree is of the order of $0.1 \mu\text{Hz}$, and consequently, they argued, the spectrum could not be resolved into individual modes. They did not, however, explain why radial modes should stand above this quasi-continuum, which would appear to be necessary for explaining Buzasi's observations. Moreover, they failed to point out that a g mode that resonates at a corresponding (i.e., same value of ℓ) characteristic p-mode frequency of the outer acoustic cavity can have a particularly large amplitude at the surface.

3.1 General properties

The basic properties of nonradial oscillations in highly evolved stars were determined in the 1970s (Dziembowski, 1971, 1977; Osaki, 1977). However, the objects of interest in those early works were stars in the Cepheid instability strip. To the best of our knowledge there is only one paper devoted to the theory of nonradial oscillations in red giants. It is a short note by Keeley (1980), in which a crude estimate of mode trapping was made. The nonadiabatic effects, which are very important in this context, were ignored.

The differences in the nonradial mode properties between red and yellow giants are a consequence of the different depths of the convection zones. The formalism for calculating linear modes in these two types of star is the same. Here we provide only an outline of the formalism developed by Dziembowski (1977), which was recently recalled in some detail by Van Hoolst et al. (1998, hereafter VDK). We intend to apply this formalism to low-degree modes ($\ell = 1, 2$), in a cyclic-frequency range starting somewhat below the fundamental radial-mode frequency and extending up to the acoustic cut-off frequency, ν_{ac} , in the photosphere ($r = R$). In our model of α UMa, $\nu_{\text{ac}} \simeq 27 \mu\text{Hz}$. Buzasi et al. (2000) reported peaks in the power spectrum located above our value of ν_{ac} , which evidently cannot easily be interpreted in terms of strongly trapped acoustic modes.

The starting point of our discussion is an asymptotic solution, for large order n , of the nonadiabatic wave equation, which is valid in the radiative interior. In this approximation, any perturbed scalar parameter may be expressed with respect to spherical polar coordinates (r, θ, ϕ) in the following form:

$$q(r, \theta, \phi, t) = A(r) [e^{i\Phi(r)} + e^{-i\Phi(r)}] Y_\ell^m(\theta, \phi) e^{i\omega_c t}, \quad (1)$$

in which t is time. The amplitude, A , is a slowly varying function of r . The rapid variations are described by the

phase Φ , which for stars with radiative cores may be written in the form

$$\Phi(r) = \int_0^r k dr - \frac{1}{2}(\ell + 1)\pi. \quad (2)$$

The general expression for the radial component, k , of the wave number of high-order modes in the gravity-wave cavity may be found in VDK. The quantity $\omega_c = \omega - i\gamma$ (with $\omega > 0$) is the complex eigenfrequency. We focus our attention on predominantly oscillatory modes, i.e. modes with a growth rate γ satisfying the condition $|\gamma| \ll \omega$. We also specify q to be the relative Lagrangian perturbation to the pressure, $\delta p/p$.

If the radiative energy losses are regarded as being small, there is a simple expression for the radial wave number far from the edges of the cavity:

$$k \simeq \frac{\sqrt{\ell(\ell+1)}}{\omega} \frac{N}{r} [1 + i(\mathcal{D} + \frac{\gamma}{\omega})], \quad (3)$$

where

$$N = g \sqrt{\left(\frac{dp}{dr} - \frac{\rho}{\Gamma_1 p} \right)} \quad (4)$$

is the buoyancy (Brunt-Väisälä) frequency, g is the local gravitational acceleration, ρ is density, $\Gamma_1 = (\partial \ln p / \partial \ln \rho)_{\text{ad}}$ is the first adiabatic exponent, and

$$\mathcal{D} = \frac{\ell(\ell+1)}{8\pi\omega^3} \frac{gL_r}{r^4 p} \frac{\nabla_{\text{ad}}}{\nabla} (\nabla_{\text{ad}} - \nabla), \quad (5)$$

in which $L_r(r)$ is the total rate at which radiant energy crosses a sphere of radius r , $\nabla = d \ln T / d \ln p$ and $\nabla_{\text{ad}} = (\partial \ln T / \partial \ln p)_{\text{ad}}$. The quantity \mathcal{D} is a measure of the radiative energy loss, which is the only nonadiabatic effect we consider in this cavity. Here, $\nabla_{\text{ad}} > \nabla$ is always satisfied; hence $\mathcal{D} > 0$. To the same approximation, the amplitude is given by

$$A(r) \propto \frac{V}{r^3 \sqrt{k\rho}}, \quad (6)$$

with $V = g\rho p / p$. The approximate expressions for the wave number (equation 3) and for the amplitude (equation 6) are valid only if $\mathcal{D} \ll 1$. For models M23 and M24 (see Table 1) the computations suggest that $\mathcal{D} \gg 1$ in certain layers inside the star, at least for some modes considered in the calculations. However, for these models we use this approximation only in the outer layers of the asymptotic region, where the approximation is satisfied. The maximum value of \mathcal{D} in our model of α UMa for the lowest-frequency quadrupole ($\ell = 2$) mode is 0.2. As in all red-giant models, that maximum occurs within the shell source. Even if \mathcal{D} is

small, consequences of radiative losses may still be very important for the wave properties, because if N/ω is large we may still have $\Phi_i \equiv \Im(\Phi) \gg 1$. Equation (1) describes a superposition of an outward (first term on the rhs) and inward propagating gravity wave, where the direction of propagation is the direction of the group velocity.

Let us concentrate now on the oscillations in the outer, acoustic cavity. Moreover, let us assume that the approximation for q given by equation (1) is valid in an interval $[0, r_f]$ of the g-mode cavity. In this interval we can neglect the derivative of A with respect to r in the calculation of the derivative of q . Thus, at $r = r_f$ we have approximately

$$\frac{1}{q} \frac{\partial q}{\partial r} = ik \frac{\exp(i\Phi) - \exp(-i\Phi)}{\exp(i\Phi) + \exp(-i\Phi)}, \quad (7)$$

which provides a boundary condition for the numerical solution of the equation for the linear nonadiabatic oscillations in the interval $[r_f, R]$, which contains the very outer layers of the g-mode cavity in which the asymptotics breaks down, the entire surrounding acoustic cavity and the evanescent zone between. The lhs of equation (7) depends on ℓ and on the value of ω_c . The dependence on ω_c is relatively weak in comparison with the explicit dependence of the rhs of equation (7).

Assuming $\Phi_i \gg 1$, expression (7) simplifies to

$$\frac{\partial q}{\partial r} \simeq -ikq, \quad (8)$$

which is valid for the case when the wave is effectively dissipated on its way towards the centre. The energy loss may be overcompensated by the driving operating in the outer layers if the wave amplitude $A(r_f)$ is small, i.e., if the mode trapping in the acoustic propagation zone is severe. Indeed, nonradial modes with growth rates γ similar to those of radial modes were found in models of Cepheids (Osaki, 1977) and of RR Lyrae (Dziembowski, 1977). In these two independent papers, equation (8) was used for the inner boundary condition. Such modes were named in VDK as S(trongly) T(rapped) U(nstable). We must emphasize, however, that even when the amplitude in the outer acoustic zone is relatively large, according to VDK the oscillations typically have 80% of their energy in the inner, g-mode cavity. In the model of the RR Lyrae star considered by VDK, STU modes were found only with $\ell > 4$. We shall see that in red giants STU modes may exist also with ℓ as low as unity. The frequency separation between consecutive low-degree STU modes is similar to the separation between consecutive radial modes.

The STU modes are true eigensolutions of the nonadiabatic oscillation equations for the whole star. Indeed, the boundary conditions (7) and (8) are equivalent for unstable modes because if $\gamma > 0$ we have $\Im(k) > 0$ throughout the interval $[0, r_f]$, and Φ_i does not change sign. If $\mathcal{D} \ll 1$, this conclusion follows immediately from equation (3) although, in fact, it is true also for any $\mathcal{D} \geq 0$ (see e.g. Dziembowski, 1977). For stable modes, the situation is more involved. If a solution with $\gamma < 0$ is found subject to the inner boundary condition (8), then the solution must always be checked to determine whether it satisfies the inequality $\Phi_i \gg 1$. Actually, this inequality is rarely satisfied. Let us note that with the usage of equation (7) we assume maximum energy losses. When we use equation (7) with a properly calculated phase,

instead of equation (8), we may find unstable modes. However, for such modes the growth rates are typically much smaller than those of radial modes with similar frequencies.

A dense spectrum of weakly unstable modes with $\ell = 1$ and 2 was found for the RR Lyrae model considered by VDK. We shall discuss in the next Section the problem of mode stability, and we shall see that it is actually far from being solved. Fortunately, whatever the mechanism responsible for the excitation of the modes, it should operate in the layers where the radial eigenfunctions do not depend on ℓ . We shall take advantage of this property in our discussion of the relative chances of nonradial or radial modes being excited.

It seems to be not unreasonable to assume that if in a certain frequency range unstable modes of various degrees exist, their chances of being excited are related to the growth rates γ . The growth rate may be expressed in terms of the work integral, W , and the mode inertia, I , through the well-known relation (see e.g. Unno et al. 1989)

$$\gamma = \frac{W}{2\omega I}. \quad (9)$$

The generic expression for the work integral is

$$W = \int d^3x \rho [-T \nabla_{\text{ad}} \Im(q^* \delta s)] + \int d^3x \Im \left(\frac{\delta \rho^*}{\rho} \frac{\delta p_t}{p_t} \right), \quad (10)$$

where s is the entropy per unit mass and p_t (the so-called turbulent pressure) is the rr -component of the Reynolds stress tensor $T_{ij} \equiv \overline{\rho u_i u_j}$ (u is the turbulent velocity field and the overbar denotes an ensemble average). The asterisk denotes complex conjugate. In this expression we neglect the contribution from the anisotropy of the Reynolds stress tensor, which is small compared with the isotropic component. But in this section we neglect convection dynamics in the model computations: in the evaluation of the work integral the second term of the rhs of equation (10) is neglected. The mode inertia is defined as

$$I = \int d^3x \rho |\xi|^2, \quad (11)$$

with ξ representing the displacement eigenfunction. The integrals are over the entire volume of the star. The inertia I enters also into the expression for the amplitudes of stochastically excited modes (see equation 21). Another quantity in the expression for the amplitudes is the energy supply rate P_Q injected into the modes by the turbulent convection, and which we assume to be generated predominantly by the fluctuating Reynolds stresses (see next Section).

There are important differences between radial and nonradial oscillation properties below the acoustic propagation zone of the nonradial modes. These differences are reflected in the values of I . If I is large, the largest contribution to the work integral may arise in the gravity-mode propagation zone, where the asymptotic approximation is applicable. In the gravity-wave propagation zone we have adopted for the Lagrangian specific entropy perturbation the expression

$$\delta s = 2i c_p \left(\frac{\partial \ln T}{\partial \ln \rho} \right)_p \left(\frac{d \ln p}{d \ln \rho} - \frac{1}{\Gamma_1} \right) \mathcal{D} q, \quad (12)$$

in which c_p is the specific heat at constant pressure. It follows, for example, from equation (19) of VDK in the weakly

nonadiabatic limit, that is, when $|\mathcal{D}| \ll 1$. Substituting equations (1) and (12) into equation (10) we obtain

$$W_g = -2C_f \omega^2 \int_0^{\Phi_{r,f}} h \mathcal{D} d\Phi_r, \quad (13)$$

where $\Phi_r \equiv \Re(\Phi)$ and C_f is a real positive constant which is obtained from the eigenfunctions calculated numerically for $r > r_f$, and

$$h = \exp(2\Phi_i) + \exp(-2\Phi_i). \quad (14)$$

The oscillatory term, proportional to $\cos(2\Phi_r)$, in the integrand of W_g has been ignored, which is consistent with the asymptotic approximation.

An expression for ξ in terms of q can be calculated in the adiabatic approximation. The result is

$$\xi = -\frac{r}{V} \left[q \mathbf{e}_r + \frac{r^2}{\ell(\ell+1)} \nabla_h \left(\frac{\partial q}{\partial r} \right) \right], \quad (15)$$

where \mathbf{e}_r is a unit vector in the radial direction and ∇_h is the horizontal component of the gradient operator. From equation (3) we conclude that, to a first approximation, the contribution of the radial displacement to I can be neglected if $N \gg \omega$. Thus, from the asymptotic interior we obtain the following contribution to the modal inertia I :

$$I_g = C_f \int_0^{\Phi_{r,f}} h d\Phi_r. \quad (16)$$

We normalize the relative rms radial component of the mode displacement to unity at the stellar surface. The coefficient C_f , which is a function of ω , exhibits minima separated by nearly the same interval in frequency as the minima in the radial modes. This is a manifestation of the trapping properties of the acoustic cavity, which are purely dynamical and result from a resonance between the two cavities. The spectrum of g modes in the inner cavity is so dense that there is always a g-mode-like oscillation whose frequency resonates with a p mode in the outer cavity, such that the amplitudes in both cavities are similar. All other g modes are confined to the central g-mode cavity, and have very low amplitudes in the outer layers of the star. Mode trapping is influenced also by the behaviour of the factor h (see equation 14), which is determined by nonadiabatic effects. For STU modes we have $h \approx \exp(2\Phi_{i,1}) \gg 1$, which is a sharply increasing function of r . Thus, I_g is negligible and W_g may be evaluated as the rate of wave losses:

$$W_{g,w} = - \left(r^2 p \int \Im(\xi_r^* q) \sin \theta d\theta d\phi \right)_f = -C_f \omega^2 h_f. \quad (17)$$

For all other modes we have to use equations (13) and (16) to evaluate the contributions W_g and I_g . Equation (3) implies that for stable modes $h(r)$ has a maximum in the layer in the star in which $\mathcal{D} = -\gamma/\omega$. Thus, I_g may be a significant, and is often the dominant contribution to I . Let us note that the values of I_g and W_g depend on γ , and consequently on the nonadiabatic processes operating in these layers. This means that uncertainties in the computation of the nonadiabatic effects are to some degree reflected in the values of I_g and W_g . Damping in the outer layers reduces the effect of mode trapping.

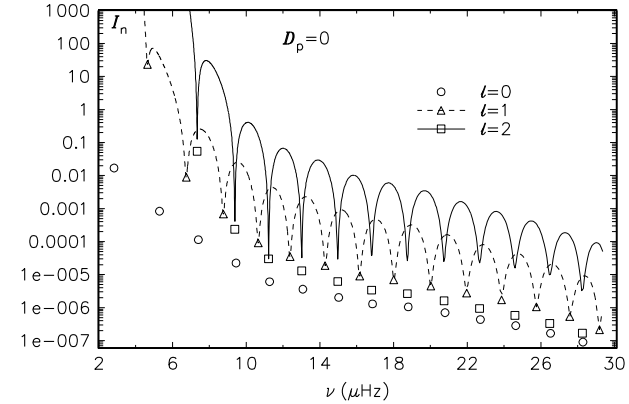
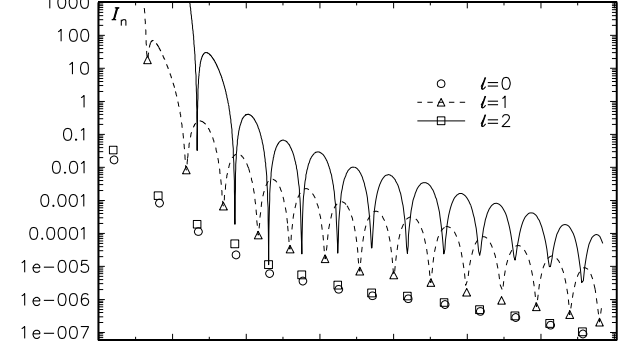


Figure 2. Modal inertia in units of $3MR^2$, plotted against frequency. The eigenfunctions are normalized such that at the surface $\xi_r = R Y_l^m(\theta, \phi) \exp(i\omega_r t)$. Individual nonradial modes are not resolved. The symbols are displayed only for those modes that are locally most trapped. $D_p = 0$ means that all nonadiabatic effects in the outer layers are ignored.

3.2 Application to α UMa

In our code for computing nonradial nonadiabatic oscillations (Dziembowski, 1977) we set the Lagrangian perturbation of the turbulent fluxes (heat and momentum) to zero, and we ignore the turbulent pressure in the equilibrium model. With this treatment, all radial modes are found to be unstable.

In Fig. 2 we show the behaviour of the normalized mode inertia $I_n = I/3MR^2$ as a function of the cyclic frequency $\nu = \omega/2\pi$ for our model of α UMa. The choice of normalization is not important here, except that all modes are assumed to have the same surface amplitude of radial displacement. There are two sequences of model results: in the first sequence (upper plots) we calculated h with γ obtained from our code; in the second sequence we suppressed all nonadiabatic effects where $r > r_f$. A comparison allows us to assess some of the consequences of the uncertainties of the physics in the convective zone.

Symbols are used to denote the nonradial modes that are most trapped in the acoustic cavity. For the $\ell = 2$ sequence the minima in I_n almost coincide with the radial-mode frequencies, while the minima for $\ell = 1$ are located roughly half-way between the $\ell = 0$ and $\ell = 2$ minima. The positions of these minima resemble the positions of modes in the whole-disc spectra of solar oscillations. There are many more modes with $\ell = 1$ and $\ell = 2$ than are depicted by the

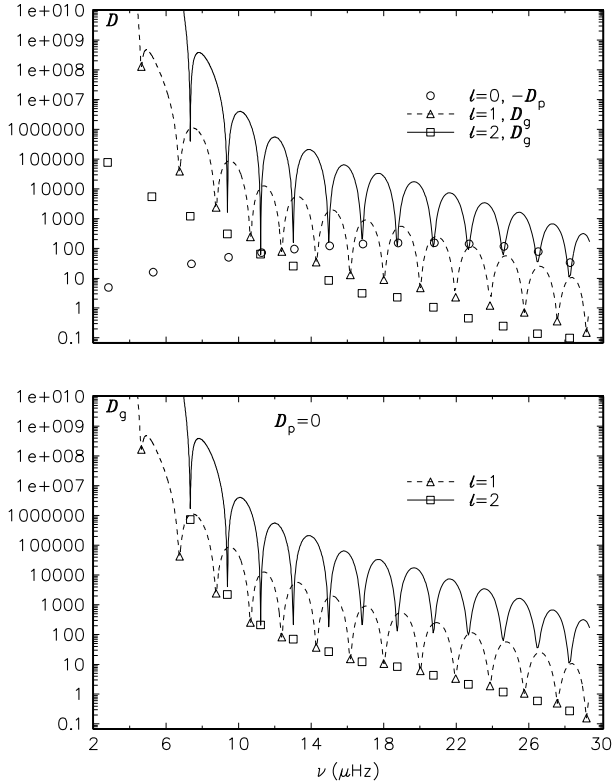


Figure 3. Contributions to the energy dissipation rate from the g-mode propagation zone in units of the stellar luminosity, L . In the upper panel the energy gain rate for radial modes is plotted with open circles. See caption of Fig. 2 for further information.

symbols. The frequency separation $\Delta\nu$ between nonradial modes of consecutive order n is indeed very small. It may be evaluated from the asymptotic formula

$$\frac{\Delta\nu}{\nu} = 2.4 \times 10^{-4} \frac{\nu}{\sqrt{\ell(\ell+1)}}, \quad (18)$$

where ν is expressed in μHz . The numerical constant is specific to the model. At $\ell = 1$ and $\nu = 2.8\mu\text{Hz}$ the value of $\Delta\nu$ is about $0.0013\mu\text{Hz}$, much less than that found by Guenther et al. (2000).

There is no substantial difference between the trapping pattern of the two sequences, except for the differences in the depths of the minima, particularly those of the $\ell = 2$ modes. Greater driving in the outer layers results in deeper minima. If there is net damping in the outer layers, as in the case of solar oscillations, the minima are shallower than in the adiabatic approximation.

In Fig. 3, we plot the rate of energy dissipation, $D_g \equiv -\omega W_g$, in the asymptotic interior for the same two sequences of modes. In addition, in the upper panel, we show the total energy gain rate, $-D_p \equiv -\omega W$, for radial modes. The total driving rate for the nonradial modes is given approximately by $\gamma \simeq (D_p(\nu) + D_g)/2\omega^2 I$, because significant nonadiabatic effects may arise only either near the surface—and then they are ℓ -independent—or in the deep interior where the g-mode asymptotics applies. Some nonradial modes with frequencies larger than $12\mu\text{Hz}$ are found to be unstable: if the radial modes with $\nu > 12\mu\text{Hz}$ are indeed unstable, then there are also some unstable low-degree nonradial modes.

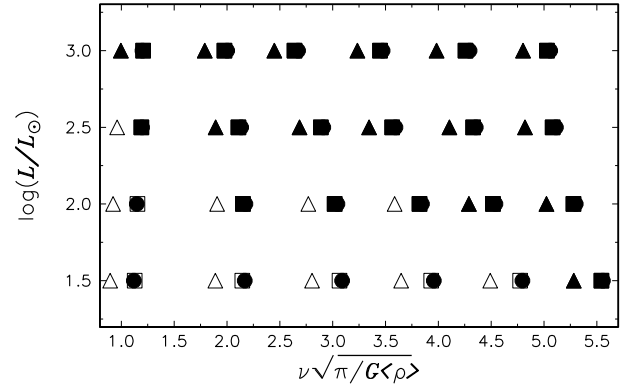


Figure 4. Occurrence of instability in the sequence of $2 M_\odot$ giants of nonradial mode of low degree l and low radial order n that are most strongly trapped in the outer acoustic cavity. The abscissa is the dimensionless frequency $\sqrt{\pi/G \langle \rho \rangle \nu}$. Full symbols denote unstable modes, open symbols stable modes. Circles, triangles, and squares denote $\ell = 0, 1, 2$ modes, respectively

When $\ell = 2$ the modes that are most trapped are detached from the remaining modes, except for the one at $\nu \simeq 10\mu\text{Hz}$. Except for this particular mode, all the other modes satisfy $\Phi_{i,f} > 1$. Thus, the unstable $\ell = 2$ modes are STU modes, and their growth rates are nearly the same as those of the corresponding radial modes. All the unstable $\ell = 1$ modes have $\Phi_{i,f} \ll 1$, and the trapping effect is less severe. The inertiae of the most trapped $\ell = 1$ modes are always significantly larger than those of the closest radial mode (see Fig. 2).

3.3 “Unstable” low-degree modes in $2 M_\odot$ red giants

In Table 2 we compare some characteristics of modes of the α UMa model, M_α , and the modes of models of $2 M_\odot$ red giants that are found to be unstable with our code. For the models M21 and M22 we find more-or-less similar properties to those of the M_α model. Strong trapping occurs only for $\ell \geq 2$, and the nonradial modes are unstable for the higher n . Note that n is the radial order only for $\ell = 0$ (for $\ell > 0$ it is the number of nodes in the acoustic cavity of the radial component of the displacement eigenfunction). For all cases the upper limit of the unstable range is determined by the acoustic cut-off frequency.

In the more luminous giants (models M23 and M24) STU modes are found even for $\ell = 1$. In Fig. 4, we show how instability of the most strongly trapped modes increases with stellar luminosity.

The relative frequencies of the most strongly trapped modes of the models considered here are different from those of the RR Lyrae star model considered by VDK and of RR Lyrae stars in general. In red giants the most strongly trapped $\ell = 1$ modes are located between the $\ell = 0$ and $\ell = 2$ pairs, whose frequencies are nearly coincident. There is a similarity with solar p modes, although in the case we have studied here the frequencies of the strongly trapped $\ell = 1$ modes are somewhat closer to the higher-frequency even-degree pair. In RR Lyrae stars, on the other hand, the frequencies of the most strongly trapped $\ell = 1$ modes are

Table 2. “Unstable” low-degree modes in red-giant models; ν_{ac} is the cyclic acoustic cut-off frequency computed for an Eddington grey atmosphere; $\Pi_{0,1}$ is the period of the fundamental radial mode; for $\ell > 0$, n indicates the range of consecutive modes that are most trapped.

Model	ν_{ac} μHz	$\Pi_{0,1}$ days	n-range			ν -range (μHz)		
			$\ell = 0$	$\ell = 1$	$\ell = 2$	$\ell = 0$	$\ell = 1$	$\ell = 2$
M_{α}	26.6	4.10	1-14	8-14	4-12	2.82-26.3	16.2-27.7	15.0-28.2
M21	178.	.919	1-18	6-18	6-18	12.6-166.	59.5-162.	62.5-166.
M22	43.4	2.65	1-13	5-14	3-13	4.36-40.3	16.3-41.9	11.5-40.3
M23	10.2	7.74	1-9	2-10	1-12	1.50-9.30	2.37-9.81	1.49-10.1
M24	2.25	24.1	1-6	1-6	1-6	.480-2.03	.397-1.92	.483-2.01

actually closer to the radial eigenfrequencies than are the frequencies of the most strongly trapped $\ell = 2$ modes.

These differences between RR Lyrae stars and red giants are related to red giants having much deeper convective zones. The differences are reflected in the different behaviours of the Brunt-Väisälä frequency, N . In Fig. 5 we compare N and the Lamb frequencies L_1 and L_2 in the envelope of an RR Lyrae model with those in the envelope of model M21. A deeper convective zone is associated with a wider evanescent zone separating the p-mode and g-mode propagation zones, and hence there is a possibility of more efficient trapping. This is why we find STU modes of low degree in red-giant and not in RR Lyrae models. Exceptionally poor trapping of the $\ell = 2$ modes in the frequency range of the first two radial modes is due to the narrowness of the evanescent zone.

4 EXCITATION MECHANISMS

There is little doubt that the interaction between pulsation and convection plays an essential role in red-giant pulsation, and that the approach adopted by us to obtain the results reported in the previous sections is inadequate. The driving agent that caused instability of the radial modes is the same as that suggested first by Ando and Osaki (1975) in an attempt to explain solar p-mode excitation in the Sun, and is artificial. It is easy to understand why: at the photosphere, where the energy is carried mostly by radiation, the flux perturbation is negative in the high-temperature phase of the pulsation cycle. This is a result of the steep increase of the opacity with temperature in the outer layers. The fraction of the energy carried by convection increases rapidly inwards. Since, *by assumption*, the convective flux remains unperturbed, the energy is forced to be captured by the photospheric layers, and the putative heat engine works. This phenomenon is sometimes called convective blocking, which is confusing because what actually blocks the heat flux is the opacity variation. However, there is no physical justification for the neglect of the perturbed convective heat flux and Reynolds stresses. Indeed, pulsational modulation of the convectively unstable stratification of the star is bound to modulate the convective dynamics, and dominate the driving or damping in regions where the convective fluxes dominate in the equilibrium state.

Effects of convection on the stability of radial pulsations in cool stars have been investigated since the early 1970s (see e.g. Xiong et al. 1998; Houdek, 2000). Recent efforts have focused mainly on Mira stars and the Sun. Ac-

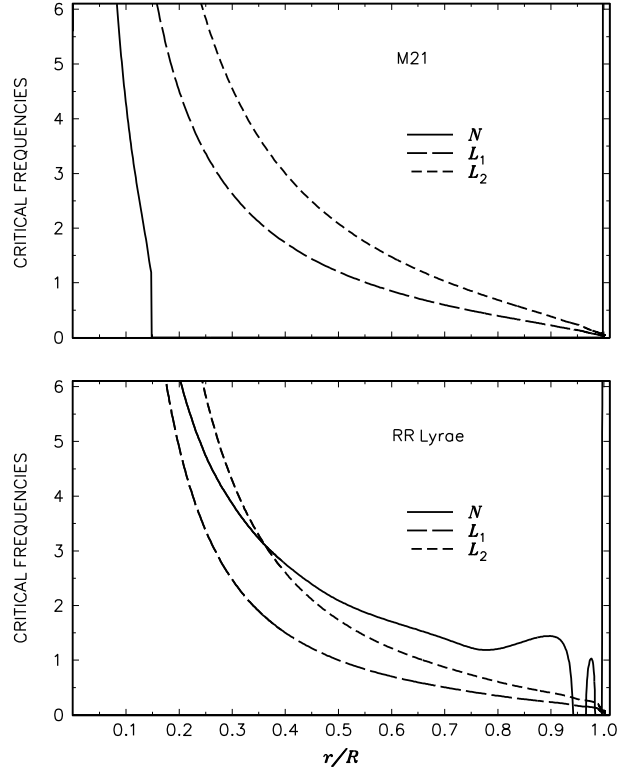


Figure 5. Lamb frequencies $L_{\ell} = \sqrt{\ell(\ell+1)c/r}$ (for $\ell = 1$ and 2) and the Brunt-Väisälä frequency N in the M21 model and in a representative RR Lyrae star model. The latter is characterized by the following parameters: $M = 0.67M_{\odot}$, $Y_0 = 0.243$, $Z = 0.001$, $Y_{\text{C}} = 0.17$ (helium abundance in the core), $\log(L/L_{\odot}) = 1.717$, $\log T_{\text{eff}} = 3.822$. The ordinate scale is dimensionless, and corresponds to angular frequencies measured in units of $\sqrt{4\pi G \langle \rho \rangle}$, which corresponds to the dimensionless cyclic frequencies of Fig. 4. In these units the frequencies of the first two radial modes in the RR Lyrae model are 1.82 and 2.46.

cording to the calculations of Xiong et al. (1998), low-order radial modes of Mira models are unstable, whereas those of orders $n > 4$ were always found to be damped (see also the work by Balmforth et al. (1991) on Arcturus). In a study of p-mode stability in the Sun by Balmforth (1992a), all modes have been found to be stable. Balmforth used in his calculations Gough’s (1976, 1977) nonlocal, time-dependent mixing-length model for convection, improving on the code used by Baker & Gough (1979) to study RR Lyrae stars by incorporating the Eddington approximation to radiative transfer for both the equilibrium structure and the pul-

sations. Houdek et al. (1999) applied these calculations to solar-type stars, and estimated amplitudes of intrinsically stable stochastically excited radial oscillations in stars with masses between $0.9 M_{\odot}$ and $2.0 M_{\odot}$ close to the main sequence.

4.1 Linear stability of radial modes in α UMa

Here we apply Balmforth's (1992a) treatment of pulsation to a model of α UMa. In particular, we include turbulent pressure in the equilibrium model, and the stability analysis includes the Lagrangian perturbations of the convective heat and momentum fluxes. We use an envelope model calculated with the surface parameters of model M_{α} given in Table 1, and an atmosphere using the T - τ relation of model C of Vernazza, Avrett & Loeser (1981). The value of the mixing-length parameter was adjusted such as to reproduce the same depth of the convective zone as was obtained from the evolutionary computation. The nonlocal treatment of convection introduces two more parameters, a and b , which characterize respectively the spatial coherence of the ensemble of eddies contributing to the total heat and momentum fluxes and the extent over which the turbulent eddies experience an average of the local stratification. Theory suggests approximate values for these parameters, but it is arguably better to treat them as free. Roughly speaking, the parameters control the degree of 'nonlocality' of convection; low values imply highly nonlocal solutions, and in the limit $a, b \rightarrow \infty$ the system of equations reduces to the local formulation (except near the boundaries of the convection zone, where the local equations are singular).

The energy dissipation rate D_p of radial p modes was calculated as a continuous function of oscillation frequency by relaxing the inner dynamical boundary condition. The results shown in the upper panel of Fig. 6 were obtained for two sets of the nonlocal convection parameters a and b . The choice of these parameters is important at high frequencies where unstable frequency ranges are found. At low frequency, covering radial orders up to $n = 5$, all modes are found to be stable for both sets of the a and b parameters. The values of $|D_p|$ are significantly higher than the values of $-D_p$ shown in the upper panel of Fig. 3. This clearly indicates that by neglecting the perturbed convective fluxes we ignore the dominant contribution to the damping.

The results shown in Fig. 6 are applicable also to non-radial modes, because virtually all the contribution to D_p arises in the upper layers where the value of ℓ has little influence. However, damping effects in these layers have consequences in the deep interior. They change γ , and hence the amplitude behaviour in the g-mode propagation zone (see equation 3). We have seen in Section 3.2 (Figs. 2 and 3) that ignoring driving effects in these layers reduces the trapping. Adding damping there would reduce it further. Larger inertiae imply lower amplitudes for stochastically excited modes, and indeed we should not expect a detection of stochastically excited nonradial modes in giants.

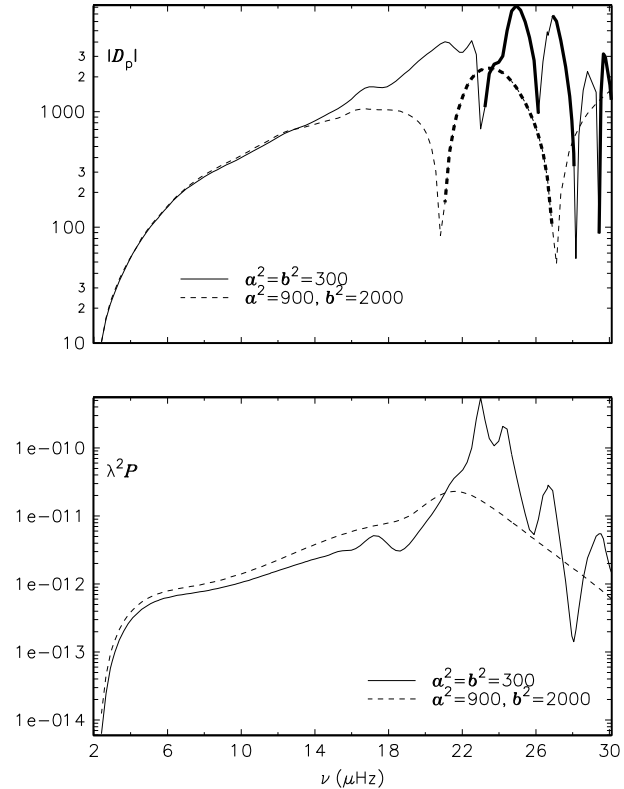


Figure 6. Absolute values of energy dissipation rates, $|D_p|$ (top) and energy generation rate $P\lambda^2$ (bottom) (P is the rate of energy injected into the modes by the fluctuating Reynolds stresses and λ is defined by equation 22). The energy generation rates are expressed in units of the solar luminosity. Two sets for the convection parameters a and b were used. Thick curves in the upper panel indicated the frequency range where radial modes are found to be unstable ($D_p < 0$).

4.2 Amplitudes of stochastically driven radial modes

The amplitudes of intrinsically stable stochastically driven radial modes were estimated in the manner of Houdek et al. (1999):

$$V_s = \sqrt{\frac{P_Q}{2\eta I_{\omega}}}, \quad (19)$$

where here P_Q is the noise generation rate injected into a mode through the fluctuating Reynolds stresses, the expression for which we adopted from Balmforth (1992b) (see also Houdek et al. 1999). The damping rate is $\eta = D_p/2I_{\omega}^2 = -\gamma$, and $I_{\omega} = IR^{-2}$ in our notation. For radial modes the total energy dissipation rate D is D_p . The linear stability analysis also provides the parameter λ , which is the ratio of the relative luminosity to the relative velocity amplitude, computed at the surface (i.e. outermost meshpoint) of the star. The bolometric relative luminosity amplitude then becomes

$$\frac{\delta L}{L} = \lambda \frac{\delta R}{R} = \lambda \frac{V_s}{\omega R}, \quad (20)$$

and from equation (21) we obtain,

$$\frac{\delta L}{L} = \lambda \sqrt{\frac{P}{I_{\omega} D}}, \quad (21)$$

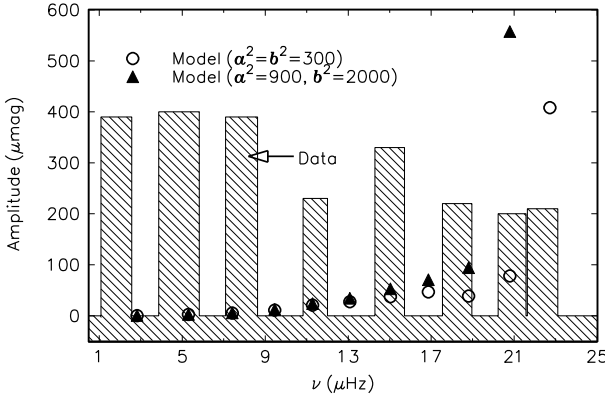


Figure 7. Amplitudes and frequencies of oscillations in α UMa from Buzasi et al. (2000) compared with model calculations obtained for two sets of convection parameters. The width of the shadowed rectangles corresponds to the uncertainty of the frequency data. Calculated amplitudes for the $n = 1, 2$, and 3 modes are $0.5, 2.7$, and $5.8 \mu\text{mag}$, respectively. The observed peaks at $\nu = 34.9 \pm 0.6$ and $\nu = 43.6 \pm 0.9 \mu\text{Hz}$, which are above the calculated acoustic cut-off frequency, are not shown.

where $P = P_Q I_n$ and $I_n = I/3MR^2$; I_n is the dimensionless modal inertia plotted in Fig. 3. In the lower panel of Fig. 6, we plot the quantity $\lambda^2 P$. All the quantities plotted in this figure are applicable also to nonradial modes of low degree. However, for nonradial modes we have to take into account the damping effects in the g-mode propagation zone. With the help of equation (21) and the data given in Fig. 3 we can evaluate amplitudes for radial modes with $D_p < 0$.

In Fig. 7, we compare radial-mode frequencies and amplitudes calculated for M_α with the observational data of α UMa. Keeping in mind the large observational errors and the fact that we have made no effort to adjust model parameters to fit the frequencies, we regard the agreement of frequencies as satisfactory. On the other hand, the disagreement between the amplitudes is very serious: the observed amplitude at $n = 1$ exceeds the predicted value by three orders of magnitude, and the frequency dependence of the amplitudes differ drastically.

An additional difficulty is presented by the presence of the two peaks above the acoustic cut-off frequency. Such high-frequency peaks are observed in the Sun, but with amplitudes much lower than those below the acoustic cut-off. The two highest-frequency peaks in α UMa have amplitudes of about $0.2 \mu\text{mag}$, which are similar to most of the other peaks. We should stress that the amplitude estimates in Fig. 7 were obtained using the pulsation modes of a model with an atmosphere based on model C of Vernazza, Avrett & Loeser (1981). That atmosphere has an acoustic cut-off frequency of $32.4 \mu\text{Hz}$ at the temperature minimum, which is lower than the two highest frequencies of the observed peaks. A more realistic atmosphere might have a higher value than this, which itself is higher than the value for the Eddington grey atmosphere quoted in Table 2 and used by Guenther et al. (2000).

The amplitudes of stochastically excited nonradial modes, including those that are most efficiently trapped in the acoustic cavity, are expected to have values much lower than those of corresponding radial modes. Equation (20) applies to nonradial modes if the contributions to I_n and D

from the g-mode propagation zone are included. The values of both I_n and D_g are substantially larger than those plotted in the lower panels of Fig. 2 and 3, owing to the damping effect in the outer layers.

5 SOLAR-LIKE OR MIRA-LIKE OSCILLATIONS ?

The results of the stability analysis presented in Section 4.1 seem to exclude an interpretation of the low-frequency part of the α UMa oscillation spectrum in terms of self-excited modes. Indeed, the damping effect of convection exceeds by a large margin the driving effect of the opacity perturbation. However, there still seems to be a greater chance for an interpretation in terms of Mira-like excitation than in terms of solar-like excitation. The trend of calculated amplitudes is determined mainly by the factor $I_n^{-1/2}$ in equation (21), which is the most reliably calculated quantity in the expression. One may contemplate that for the first three modes D_p is really much lower than what we calculated, but this option would require near cancellation of damping and driving effects; it is more plausible that the quantity is less than zero and that the modes are unstable. The option that remains is an increase of $\lambda^2 E$ by four to six orders of magnitude.

Whatever is the correct answer, the required changes are bound to be related to the way in which we treat the interaction between pulsation and convection. Our treatment, like most of those that have been used, is based on the mixing-length formalism, and we know that it is an inadequate tool for describing the mean properties of convection. In studies of acoustic mode damping and excitation we have to consider more detailed aspects of the dynamics of convection. The alternative is a hydrodynamical simulation. This has already been applied to solar radial oscillations by e.g. Stein and Nordlund (2001). It is to be hoped that before long this approach will become applicable to red-giant oscillations too.

How could future observational work on red-giant variability help us? One possibility is the disproof of genuine pulsations in α UMa and in other red giants. Short-term variability could be a direct manifestation of convection, like large-scale granulation. This would result in progress being slow: compare how much we have learned in the past from the Sun's granulation with what we have learned from its oscillations.

One very promising observational approach to the solar-like *vs* Mira-like alternatives is repeating the analysis of Cook's et al. (1997) MACHO data with a much longer time base or of extensive data from another microlensing projects such as OGLE (Udalski et al. 1997). Much improved frequency and amplitude resolution is expected. Showing that the ridges extend from a few days to hundreds of days with a continuous amplitude increase might strengthen the Mira-like interpretation.

Other observational evidence supporting a Mira-like interpretation would be the identification of nonradial modes. We have seen in Section 3 that if radial modes are unstable some $\ell = 1$ and 2 modes should be unstable too. If the modes are stable, then, as we discussed at the end of Section 4.2, nonradial modes will be excited stochastically, but

their amplitudes will be much lower than those of their radial counterparts.

It could be possible that low-order modes in α UMa are Mira-like whilst those of higher order are solar-like. This could also be the case for the multiperiodic M-type giants found by Koen and Laney (2000). In some of these stars the frequency ratio exceeds 10, and there is no doubt that the highest frequencies exceed the acoustic cut-off frequency. Two of the peaks in α UMa, as we have already noted, are also above the acoustic cut-off frequency, but that does not necessarily produce pulsational stability (cf. Balmforth et al. 2001)

Regardless of what the excitation mechanism is, the data on normal-mode frequencies will be very useful as a constraint on stellar parameters and models. Prospects of detecting nonradial modes is particularly interesting in this context.

ACKNOWLEDGEMENTS

Most of this work was carried out while WAD was a Raymond and Beverly Sackler Foundation Astronomer at the Institute of Astronomy, Cambridge. Research of WAD and RS is supported in part by the Polish grant KBN 5P03D 030 20. GH is grateful for the support of the UK Particle Physics and Astronomy Research Council.

REFERENCES

Ando H., Osaki Y., 1975, PASJ, 27, 581
 Baker N., Gough D.O., 1979, ApJ, 234, 232
 Balmforth N.J., 1992a, MNRAS, 255, 603
 Balmforth N.J., 1992b, MNRAS, 255, 639
 Balmforth N.J., Cunha M.S., Dolez N., Gough D.O., Vauclair S., 2001, MNRAS, 323, 362
 Balmforth N.J., Gough D.O., Tout C.A., 1991, in Gough D.O., Toomre J., eds, Challenges to theories of the structure of moderate-mass stars, Springer-Verlag, Berlin, Lecture Notes in Physics 388, 265
 Buzasi D., Catzarite J., Laher R., Conrow T., Shupe D., Gatier III T.N., Kreidl T., Everett D., 2000, ApJL, 532, L133
 Cook K.H., Alcock C., Alves D.R. et al. , 1997, in Ferlet R., Mailard J.P., Raban B., eds, Variable Stars and the Astrophysical Returns of Microlensing Surveys, Editions Frontieres, Gif-sur-Yvettes, p. 17
 Dziembowski W., 1971, Acta Astronomica, 21, 289
 Dziembowski W., 1977, Acta Astronomica, 27, 203
 Edmonds P.D., Gilliland R.L., 1995, American Astronomical Society Meeting, 187, 102.10
 Gough D.O., 1976, in Spiegel E., Zahn J.-P., eds, Problems of stellar convection, Springer-Verlag, Berlin, p. 15
 Gough D.O., 1977, ApJ, 214, 196
 Guenther D.B., Demarque P., Buzasi D., Catzarite J., Laher R., Conrow T., Kreidl T., 2000, ApJL, 530, L45
 Hatzes A.P., Cochran W.D., 1998, in R.A. Donahue, J.A. Bookbinder, eds, Cool Stars and the Sun, PASPCS 154, San Francisco, p. 311
 Houdek G., 2000, in: Breger M., Montgomery M.H., eds, Delta Scuti and related Stars, ASP Conf. Ser. Vol. 120, Michigan, p. 454
 Houdek G., Balmforth N.J., Christensen-Dalsgaard J., Gough D.O., 1999, A&A, 351, 582
 Keeley D., 1980, in P.A. Wayman, ed., Highlights of Astronomy 5, 497
 Koen C., Laney D., 2000, MNRAS, 311, 636
 Osaki Y., 1977, PASJ 29, 234
 Stein R.F., Nordlund A., 2001, ApJ, 546, 585
 Udalski A., Kubiak M., Szymański M., 1997, Acta Astronomica, 47, 319
 Unno W., Osaki Y., Ando H., Saio H., Shibahashi H., 1989, Non-radial Oscillations of Stars, University of Tokyo Press
 Van Hoolst T., Dziembowski W.A., Kawaler S.D., 1998, MNRAS, 297, 536, (VDK)
 Vernazza J.E., Avrett E.H., Loeser R., 1981, ApJS 45, 635
 Xiong D.R., Deng L., Cheng Q.L., 1998, ApJ, 499, 355